doi:10.1017/S1431927622001702
Microsc. Microanal. 28 (Suppl 1), 2022

Great White Pelican Mandible as Bioinspiration for Vehicle Design - Structural Bioprospecting Via X-Ray Micro-CT and Finite Element Analysis

Nicola C Thomas[1], William Harrison[1], Caroline Buttler[2] and Richard E Johnston[1]

[1] Faculty of Science and Engineering, Swansea University, Swansea, UK.
[2] Natural Sciences, Amgueddfa Cymru – National Museum Wales, Cardiff, UK.

Carbon dioxide emissions are a significant problem in the issue of rising global temperatures and climate change. Transport is responsible for 24% of global CO_2 emissions, as reported by the International Energy Agency (IEA) in 2020[1]. To stop climate change, greenhouse gas (GHG) emissions in all sectors need reducing drastically. A strategy for reducing greenhouse gases from transport is to reduce the weight of vehicles. Scientists and engineers have been turning to nature for bioinspiration for a number of years to solve societal problems.

A pelican can carry heavy loads in its beak pouch, with the weight being borne by the lower mandible functioning as a cantilever beam[2–4]. A great white pelican, *Pelecanus onocrotalus*, complete skull with upper and lower mandibles was borrowed from the collections in the National Museum of Wales, Cardiff. Here, the lower mandible is investigated as a source of lightweight yet strong design inspiration through X-ray micro-CT and Finite Element Analysis (FEA). Due to the specimen being from a museum collection, non-destructive testing was required. However, due to the length of the mandibles being 42.5 cm, the whole specimen was scanned as several sections, see fig.1. 3D visualisation, segmentation, and meshing were carried out using Amira version 2019.2 from ThermoFisher Scientific. The data revealed that sections 1-4 were mostly solid, had an elliptical shape, and were quite narrow. The first half of section 5 was similar to section 4, however, sections 6, 7, and the second half of section 5 were also elliptical in shape, but wider than the previous sections, hollow and contained struts connected to the outer walls. The struts in section 6 appeared to be arranged in distinct and repeating orientations, while in section 7 the struts were more numerous and appeared to have no distinct repeating directionality. Finite element (FE) bending analysis was conducted in ABAQUS/CAE 2019 from Simulia, Dassault Systèmes. A Poisson's ratio of 0.3 and Young's modulus of 100,000 N/m^2 (a value similar to aerospace aluminium) was assigned. The proximal end of each section was pinned, and a displacement was applied to the free end at a rate of 1% of the length of each section, with an incremental rotation of 10° (fig.2). Analysis revealed the mandible to be stiffer in the dorsoventral direction corresponding with the requirements of the pelican in terms of being able to carry heavy loads. The bending stiffness of section 6 was higher than sections 1-5, while section 7 had the highest bending stiffness but had no distinct repeated pattern of struts.

A simplified model of the cortical, along with the cortical thickness, strut structure, thickness, distance apart, and orientation, was replicated from section 6. FEA buckling tests were undertaken on models constructed with and without struts, with a Poisson's ratio of 0.3, a Young's modulus of 22 GPa (analogous to avian long bones[5]), and a displacement of 10. Tests were also carried out with struts placed in different locations (upper, middle, lower, and combinations of all three), to understand the influence of the struts in providing internal support to the overall mandible structure in order to ascertain which set of struts provided the greatest support. The strut structure and placement were found to provide support and strength to the outer cortical under buckling conditions (fig.3). Eigenvalue buckling analysis, which estimates the critical buckling load of a structure, was found to be highest when all struts (top, middle and lower) were included, an improvement of 15.1% compared with no struts. The higher the Eigenvalue, the more resistant the structure is to buckling. Excluding the all the strut option, the row of middle struts appears to contribute the greatest buckling resistance, providing an average of 14.5% greater resistance when compared to models without any struts, a combination of top and lower, or single upper or lower rows.

Nature does not waste resources, minimising use of materials for maximum benefit. Beams and tubular components for structural integrity are very common in many vehicles, large and small. Therefore, emulating the derived functional design principles of the pelican mandible for use in designing lightweight vehicle components subjected to similar loading conditions, has the potential to reduce material usage, and most importantly to reduce greenhouse gases from production and lifecycle emissions [6].

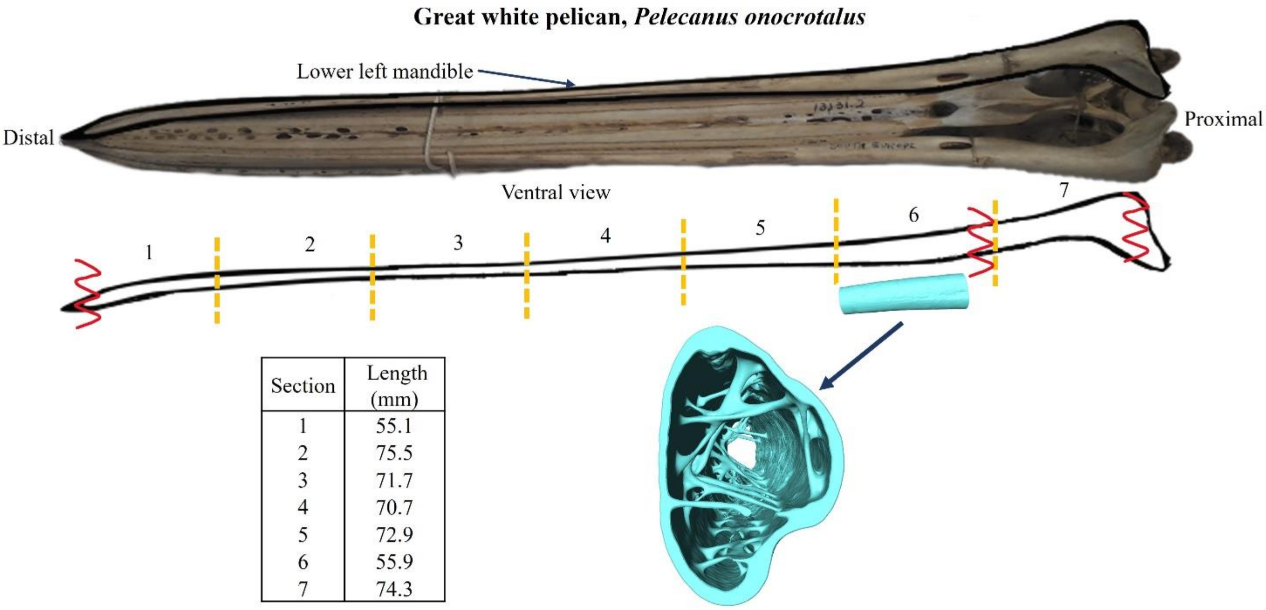

Section	Length (mm)
1	55.1
2	75.5
3	71.7
4	70.7
5	72.9
6	55.9
7	74.3

Figure 1. Diagram of the great white pelican beak, highlighting left lower mandible, allocation of sections for µCT, length of each section, and region of interest (ROI). A portion of the ROI containing a large hole was removed prior to FEA to ensure sections would be comparable.

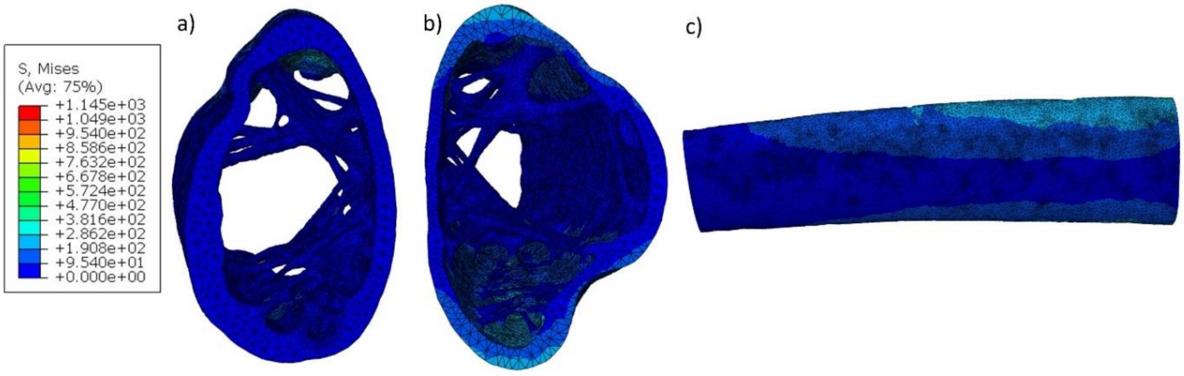

Figure 2. Finite element analysis (FEA) showing the distribution of S. mises stress on section 6 of the great white pelican lower mandible. a) distal view, b) proximal view, c) side view. Darker colours

indicate lower bending stresses, with the darkest blue indicating no stress and red highest stress measured.

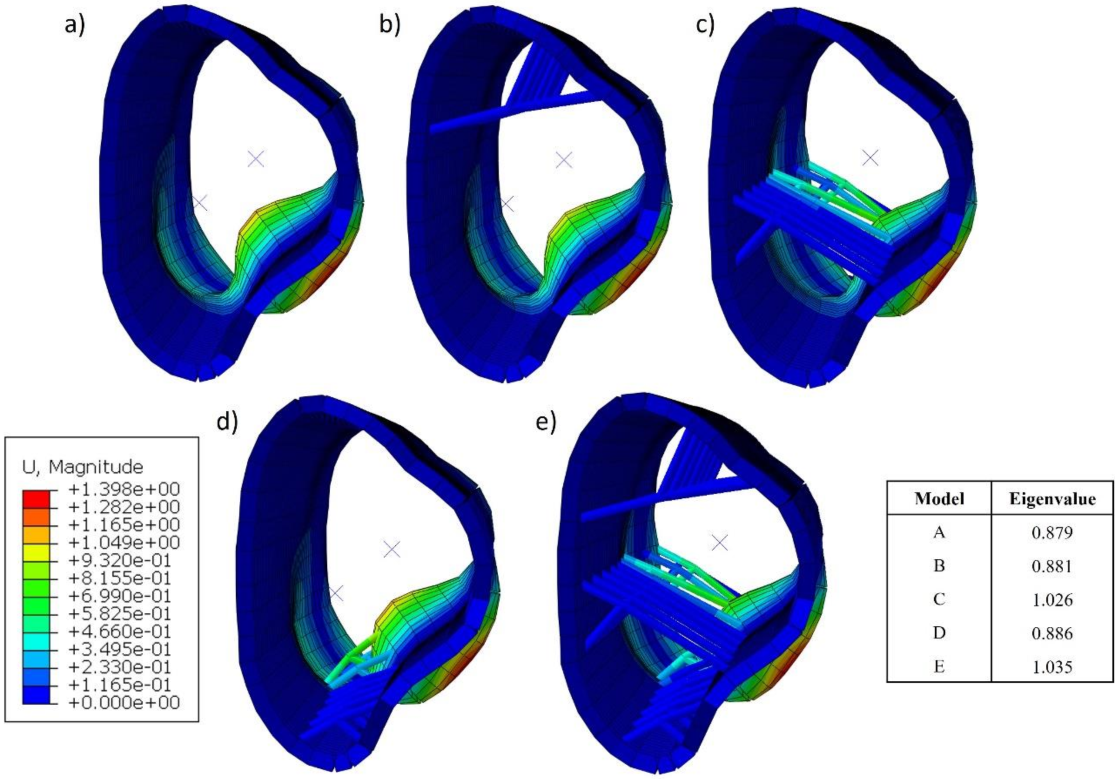

Model	Eigenvalue
A	0.879
B	0.881
C	1.026
D	0.886
E	1.035

Figure 3. Finite element analysis (FEA) showing displacement on a simplified model of the cortical shell, with struts placed in various positions: a) no struts present, b) top struts only, c) middle struts only, d) lower struts only, e) top, middle, and lower struts present. Options c) and e) have the highest Eigenvalues (higher Eigenvalues indicate greater buckling resistance), while options a), b) and d) have the lowest.

References:

[1] IEA. https://www.iea.org/reports/tracking-transport-2020 (accessed Feb 16, 2022).
[2] DJ Field et al., The Anatomical Record **294**(8) (2011), p. 1273.
[3] DJ Field et al., The Anatomical Record **293**(7) (2010), p. 1240.
[4] RA Meyers and RP Myers, The Condor **107**(2) (2005), p. 445.
[5] JD Currey, Journal of Engineering in Medicine **212**(6) (1998), p. 399.
[6] The authors acknowledge the work was supported by the Advanced Imaging of Materials (AIM) core facility (EPSRC Grant No. EP/M028267/1), the European Social Fund (ESF) through the European Union’s Convergence programme administered by the Welsh Government (80708), a Welsh Government Enhanced Competitiveness Infrastructure Grant (MA/KW/5554/19) through the European Union’s Convergence programme administered by the Welsh Government, an EPSRC Doctoral Training Award (EPSRC Grant No. EP/K502935/1), the M2A project by the European Social Fund through the Welsh Government, and support from National Museums Wales.